Quantum Electronics **46** (11) 989–994 (2016)

NONLINEAR OPTICAL PHENOMENA DOI: 10.1070/QEL16140

Extracavity and external cavity second-harmonic generation in a periodically poled silica fibre

E.I. Dontsova, S.I. Kablukov, I.A. Lobach, A.V. Dostovalov, S.A. Babin, A.V. Gladyshev, E.M. Dianov, C. Corbary, M. Ibsen, P.G. Kazansky

Abstract. **We have studied second-harmonic generation (SHG) of a cw single-frequency ytterbium-doped fibre laser, using a periodically poled silica fibre as a nonlinear medium for frequency conversion. All-fibre external cavity SHG has been investigated for the first time. A twofold increase in second-harmonic power in a fibre ring cavity has been demonstrated and possibilities of further optimising the fibre scheme have been analysed.**

Keywords: *fibre laser, second-harmonic generation, periodically poled silica fibre, quasi-phase matching.*

1. Introduction

Fibre lasers are stable and efficient light sources, a viable alternative to other types of lasers in many respects. The emission wavelength of ytterbium-doped fibre lasers (YFLs), which have a broad IR gain band, can be tuned over the range 1.03–1.15 μm (see e.g. Akulov et al. [1] and references therein). The application field of such sources can be extended by increasing their spectral range, which can be achieved using nonlinear frequency conversion. One widely used approach for extending the spectral range of lasers is second-harmonic generation (SHG).

The frequency doubling of fibre lasers can be achieved using single-pass (extracavity) and intracavity configurations with uniform (KTP and LBO) [1] and periodically poled (PPLN and PPKTP) nonlinear crystals [2]. However, the use of bulk components requires proper adjustments and increases the loss in the optical scheme. These drawbacks can be avoided by using all-fibre SHG with a periodically poled silica fibre (PPSF).

E.I. Dontsova, S.I. Kablukov, I.A. Lobach Institute of Automation and Electrometry, Siberian Branch, Russian Academy of Sciences, prosp. Akad. Koptyuga 1, 630090 Novosibirsk, Russia; e-mail: ekaterina.dontso@mail.ru;
A.V. Dostovalov, S.A. Babin Institute of Automation and Electrometry, Siberian Branch, Russian Academy of Sciences, prosp. Akad. Koptyuga 1, 630090 Novosibirsk, Russia; Novosibirsk State University, ul. Pirogova 2, 630090 Novosibirsk, Russia;
A.V. Gladyshev, E.M. Dianov Fiber Optics Research Center, Russian Academy of Sciences, ul. Vavilova 38, 119333 Moscow, Russia;
C. Corbary, M. Ibsen, P.G. Kazansky Optoelectronics Research Centre, University of Southampton, Highfield, Southampton, Hampshire, SO17 1BJ, United Kingdom

Received 19 May 2016; revision received 14 October 2016
Kvantovaya Elektronika **46** (11) 989–994 (2016)
Translated by O.M. Tsarev

It is known that silica fibres initially do not have second-order nonlinearity $\chi^{(2)}$, which can be induced by thermal poling [3, 4], and that the quasi-phase matching condition, which ensures efficient SHG, can be met by producing periodic $\chi^{(2)}(z)$ modulation along the fibre [4]. Even though the second-order nonlinearity induced in silica glass ($\chi^{(2)}_{max} \approx 0.6$ pm V^{-1} [3]) is one to two orders of magnitude lower than that in crystals ($\chi^{(2)} \approx 60$ pm V^{-1} in $LiNbO_3$ and ~27 pm V^{-1} in β-BaB_2O_4 and $KTiOPO_4$ [5]), all-fibre frequency doubling is a promising approach owing to the possibility of increasing the interaction length and integrating a nonlinear structure into a fibre scheme [6–8].

Frequency doubling of fibre laser sources in a PPSF with efficiency from 15% to 45% was demonstrated in pulsed mode at peak pump powers from 0.2 to 2 kW [7–9]. At the same time, a number of applications require compact cw visible light sources of relatively low power. In continuous mode, a PPSF was only used in a study of lasing in the yellow spectral region through the frequency doubling of a bismuth-doped fibre laser with a narrow spectrum (~0.1 nm) and ~3-W output power [10]. The highest conversion efficiency was 1.4×10^{-2}%. Compact, stable cw blue-green light sources capable of operating in both multi- and single-frequency modes are of great interest for biomedical applications. In particular, fibre lasers with frequency conversion in nonlinear crystals (see e.g. Dontsova et al. [11]) were successfully used in flow cytometry [12].

In this paper, we report the first experiments concerned with SHG in a PPSF placed in an external fibre cavity. We demonstrate that the efficiency of such an all-fibre cw blue-green light source is twice that of extracavity, single-pass ytterbium-doped fibre laser SHG. The possibilities for further efficiency improvement are discussed.

2. Fabrication of a PPSF

For this study, we fabricated a specially designed germanosilicate fibre with a core diameter of 8 μm and cutoff wavelength $\lambda_{cut} = 1.02$ μm. The fibre cladding was made of GE214 silica fibre, containing ~1 ppm of alkali metal impurities. The cladding had two holes parallel to the core and located asymmetrically with respect to the core (Fig. 1, inset). The hole diameter was 50 μm and the edge-to-edge distance between the holes was 30 μm.

The refractive index profile of the fibre along the normal to the air holes is shown in Fig. 1. Using the index profile and OptiFiber 2.0 pack (Optiwave Software), we calculated guidance characteristics of the fibre: the pump light ($\lambda_1 =$ 1030.5 nm) and second-harmonic ($\lambda_2 = \lambda_1/2 =$ 515.25 nm)

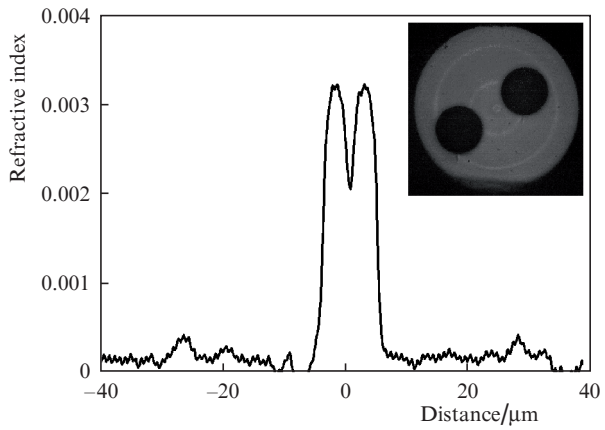

Figure 1. Transverse refractive index profile of the fibre at a wavelength of 0.63 μm along the normal to the air holes. Inset: cross-sectional electron-microscopic image of the fibre.

mode field distributions (Fig. 2a) and the effective refractive index as a function of wavelength (Fig. 2b). Note that the spectral dependence of the refractive index can be calculated analytically using known formulas. To this end, one should take into account the index dispersion in silica fibres using the Sellmeier formula [13] and the waveguide contribution to the refractive index [14]. The analytical calculation results are also presented in Fig. 2b. Over the entire wavelength range

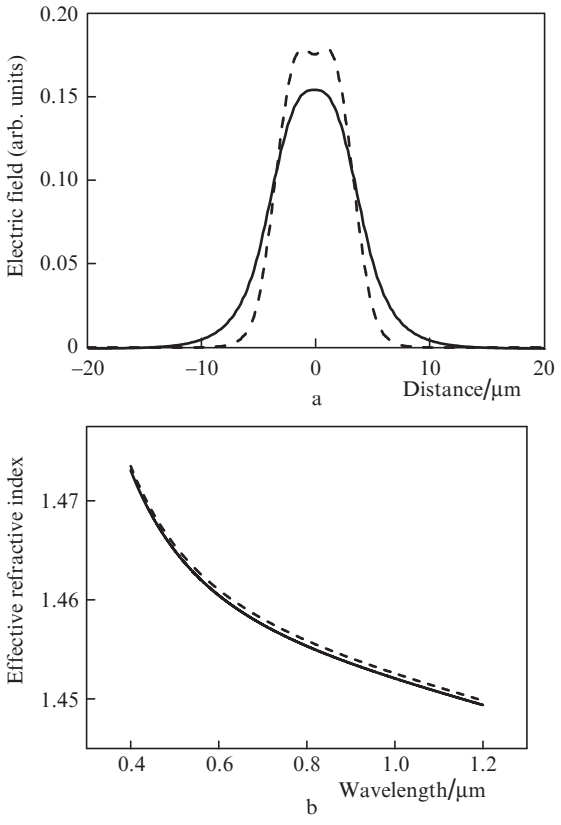

Figure 2. (a) Fundamental mode (λ_1 = 1030.5 nm, solid line) and second-harmonic (λ_2 = 515.25 nm, dashed line) field distributions; (b) dispersion of the effective refractive index of the fibre: computation with OptiFiber 2.0 (solid line) and analytical calculation by formulas from Refs [13, 14] (dashed line).

examined, the effective refractive indices in the dispersion curves obtained by the two techniques differ by $(4-6)\times10^{-4}$.

In the fibre sample under study, 17 cm in length, second-order nonlinearity was induced by thermal poling, a method described in detail elsewhere [3]. Metallic electrodes 32 μm in diameter were inserted into the holes in the fibre cladding (Fig. 3, inset) and a voltage of 8–9 kV was applied to the electrodes. The fibre, together with the electrodes, was then placed in a furnace maintained at ~220 °C. At elevated temperatures, an applied electric field shifts alkali metal ions. After cooling and removal of the external field, the persisting charge distribution in the fibre produces a strong electric field E_{DC} in the core region. The 'frozen-in' field makes the glass anisotropic and, as a result, the fibre can be thought of as a medium possessing a second-order nonlinear susceptibility: $\chi^{(2)} = 3\chi^{(3)}E_{DC}$, where $\chi^{(3)}$ is the third-order nonlinear susceptibility [4]. Given the properties of silica glass ($\chi^{(3)} = 2\times10^{-22}$ m^2 V^2, breakdown field $E_b \approx 10^9$ V m^{-1}), the upper limit of the second-order nonlinear susceptibility of silica glass can be estimated at $\chi^{(2)}_{max} \approx 0.6$ pm V^{-1}.

Phase matching necessary for efficient second-harmonic generation was ensured by periodic $\chi^{(2)}(z)$ modulation, which was produced by erasing the induced nonlinearity at equal spatial intervals with a period $\Lambda = 41.22$ μm along the length of the fibre. The nonlinearity was erased by exposing the lateral fibre surface to UV radiation at a wavelength of 244 nm, by analogy with a procedure reported by Canagasabey et al. [7]. As a result, we obtained a periodically poled silica fibre sample.

The period of the nonlinear structure, $\Lambda = 41.22$ μm, was chosen based on the quasi-phase matching condition. For the PPSF sample, it has the form

$$\Delta k(\lambda) = \beta_2 - 2\beta_1 - K_m = 0, \quad (1)$$

where $\Delta k(\lambda)$ is a generalised wave vector mismatch; $\beta_i = 2\pi\lambda_i^{-1}n_i^{eff}$ is the propagation constant; n_i^{eff} is the effective refractive index; λ_i is the wavelength of the ith harmonic; $K_m = 2\pi m/\Lambda$ is the wavenumber of the periodic structure; and m is the order of quasi-phase matching ($m = 1$ in this study).

It is worth noting that UV exposure in the PPSF fabrication process increases the optical loss in the visible spectral region. However, as shown earlier [15] this is not an obstacle to making blue-green lasers, because light in this range eliminates the UV-induced loss in the PPSF.

3. Single-pass SHG in a PPSF

Figure 3 shows a schematic of the experimental setup used to investigate all-fibre extracavity (single-pass) SHG. A pump laser beam ($\lambda_1 \approx 1.03$ μm) passes through a fibre polarisation controller and enters a PPSF sample, which is single-mode at this wavelength (cutoff wavelength $\lambda_{cut} = 1.02$ μm). Next, the transmitted pump light and generated second harmonic are separated into two channels by a wavelength-division multiplexer (WDM) for spectral and power measurements.

As a pump source, we use a single-frequency cw ytterbium-doped fibre laser with a linearly polarised output. The laser configuration in this study is similar to that described by Nikulin et al. [16]. As a master oscillator, we use a single-frequency distributed feedback (DFB) laser based on a phase-shifted long fibre Bragg grating (FBG) written into an ytterbium-doped fibre. The output power of the single-frequency source reaches 1 W and its emission bandwidth is ~1 kHz. For spectral measurements, the wavelength of the fibre laser

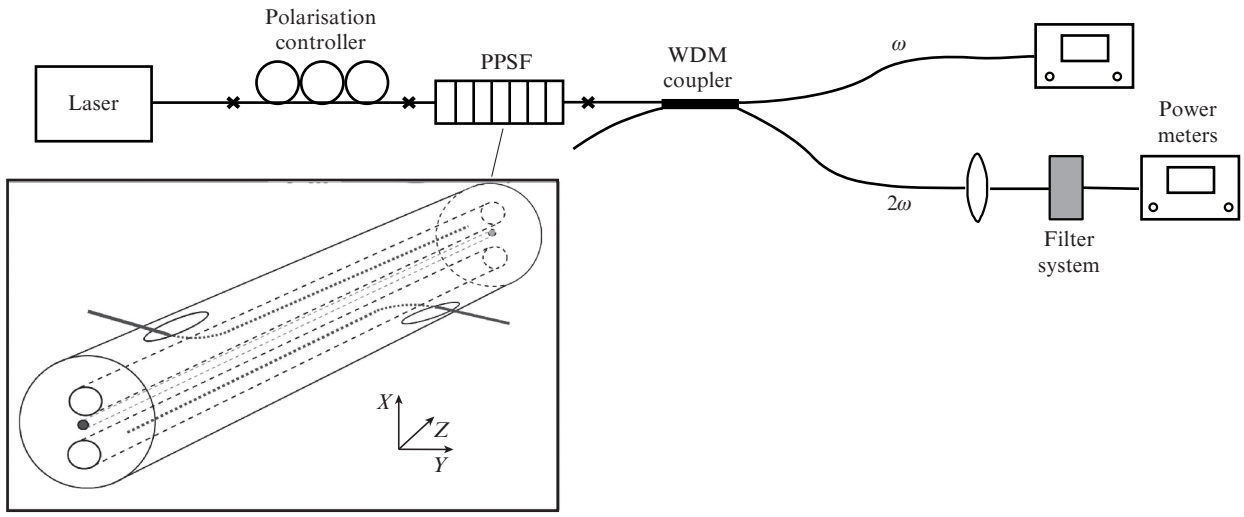

Figure 3. Schematic of the experimental setup used to investigate SHG in a PPSF sample. Inset: fibre segment for writing a periodic nonlinear structure into the sample, with the direction of its axes indicated.

can be tuned by varying the temperature of the FBG, which is placed in a separate thermostat.

SHG efficiency in PPSF samples was evaluated by measuring quasi-phase matching curves, i.e. the second-harmonic power P_2 as a function of pump wavelength (Fig. 4). Note that, to maximise the efficiency, one should take into account the polarisation properties of the PPSF. A detailed study of the spectral and polarisation properties of SHG in PPSF samples was reported by Zhu et al. [17]. A similar study was carried out by Dontsova et al. [18], using a self-sweeping fibre laser [19] as a pump source, which allowed quasi-phase matching curves to be recorded with a resolution $\delta\lambda \approx 0.3$ pm at different polarisations.

The effect of light polarisation on SHG efficiency is determined by the symmetry of the $\chi^{(2)}$ tensor. Poled silica fibres have ∞mm symmetry and, as a consequence, their $\chi^{(2)}$ tensor has three nonzero components, $\chi^{(2)}_{XXX}$, $\chi^{(2)}_{XYY}$, and $\chi^{(2)}_{YXY}$, which are in the ratio 3 : 1 : 1, respectively. (The orientation of the X and Y axes in the PPSF sample is indicated in the inset in Fig. 3.) The above symmetry properties of the $\chi^{(2)}$ tensor of poled silica fibres were confirmed experimentally by Zhu et al. [17]. Thus, to maximise SHG efficiency, not only should pump light have a certain wavelength, corresponding to the quasi-phase matching condition (1), but it should also be linearly polarised along the X axis of the PPSF sample.

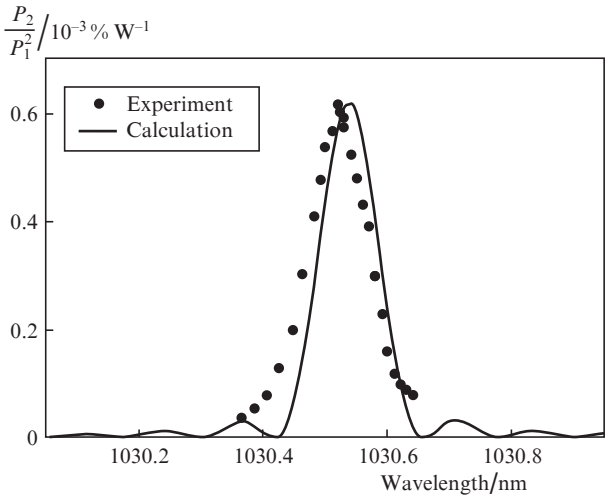

Figure 4. Normalised second-harmonic power P_2/P_1^2 as a function of pump wavelength. The experimental data were obtained with the PPSF pumped by linearly polarised single-frequency light of power P_1 = 600 mW.

In our external cavity SHG experiments in this study, we used a sample whose quasi-phase matching curve was measured previously [18] at the optimal pump polarisation (Fig. 4). The maximum measured normalised SHG efficiency was $P_2/P_1^2 = 0.62\times10^{-3}\,\%\ \mathrm{W}^{-1}$.

For a theoretical description of quasi-phase matching curves, the SHG process should be considered with allowance for the guidance properties of the fibre. This issue was addressed in detail by Risk et al. [20]. Their results demonstrate that, in the undepleted-pump regime, which was the case in our experiments, the second-harmonic power P_2 at the output of a PPSF of length L is given by

$$P_2 = \frac{\omega^2[\chi^{(2)}_{\mathrm{eff}}]^2 L^2}{2\varepsilon_0 c^3 (n_1^{\mathrm{eff}})^2 n_2^{\mathrm{eff}}} \frac{P_1^2}{A_{\mathrm{OVL}}} \operatorname{sinc}^2\left(\frac{\Delta k L}{2}\right), \tag{2}$$

where ω is the fundamental frequency; ε_0 is the electric constant; c is the speed of light; $\operatorname{sinc} x = \sin x/x$; $A_{\mathrm{OVL}} = 1/I^2_{\mathrm{OVL}}$ describes the mode overlap area at the pump and second-harmonic frequencies;

$$I_{\mathrm{OVL}} = \frac{\iint F_2(x,y)F_1^2(x,y)\,\mathrm{d}x\mathrm{d}y}{\left[\iint F_2^2(x,y)\,\mathrm{d}x\mathrm{d}y\right]^{1/2}\iint F_1^2(x,y)\,\mathrm{d}x\mathrm{d}y} \tag{3}$$

is the mode overlap integral at the pump and second-harmonic frequencies;

$$\chi^{(2)}_{\mathrm{eff}} = \frac{\iint \chi^{(2)}(x,y)F_2(x,y)F_1^2(x,y)\,\mathrm{d}x\mathrm{d}y}{\iint F_2(x,y)F_1^2(x,y)\,\mathrm{d}x\mathrm{d}y} \tag{4}$$

is the effective second-order nonlinearity averaged over the cross section of the fibre with allowance for its guidance prop-

erties; and the function $F_i(x, y)$ describes the mode field distribution of the ith harmonic in the fibre.

Formula (2) allows one to evaluate $\chi^{(2)}_{\text{eff}}$ in the PPSF sample under study from the measured normalised conversion efficiency ($P_2/P_1^2 = 0.62\times10^{-3}$ % W^{-1}) and the known guidance parameters of the sample. It should be taken into account that the input and output ends of the PPSF sample were fusion-spliced to standard single-mode fibres and that the loss per fusion splice was 1.8 dB. With allowance for the splice loss, the maximum normalised SHG efficiency directly in the PPSF was $[P_2/P_1^2]_{\text{fiber}} = 2.15\times10^{-3}$ % W^{-1}. The guidance parameters were calculated from the $F_i(x, y)$ mode field distributions (Fig. 2a) and dispersion curve (Fig. 2b): $n_1 = 1.45166$ ($\lambda_1 = 1030.5$ nm), $n_2 = 1.46416$ ($\lambda_2 = 515.25$ nm) and $A_{\text{OVL}} = 75.5$ μm^2. Thus, we find from (2) that $\chi^{(2)}_{\text{eff}} = 0.005$ pm V^{-1}.

The shape of the quasi-phase matching curve can also be modelled using (2). Using the spectral dependences of the effective refractive index in Fig. 2, we calculated the wave vector mismatch $\Delta k(\lambda)$ [see (1)] and the spectral dependence of the second-harmonic power normalised to the square of the pump power [see (2)]. Figure 4 presents, in addition to experimental data, the calculated phase matching curve for the 17-cm-long PPSF sample. In the calculation, we used the dispersion curve obtained with OptiFiber 2.0. It is worth noting that calculation with the use of the dispersion relationship and formulas from Refs [13, 14] gives similar results. It is seen in Fig. 4 that the experimental data are well represented by the theoretical curve. The slight relative shift of the peaks in the phase matching curves along the wavelength axis, by 0.019 nm, can be accounted for in terms of uncertainty in refractive index profile measurements and small transverse and longitudinal refractive index nonuniformities. The measured spectral width (FWHM) of the quasi-phase matching curve is 0.115 nm, which differs from the theoretically predicted value by just 0.008 nm.

It should be noted that the parameter $\chi^{(2)}_{\text{eff}}$ in (2) is assumed to be constant along the length of the fibre. However, the PPSF fabrication process is such that the second-order nonlinearity varies periodically along the length of the sample between zero and a maximum value $\chi^{(2)}_0$. Under the assumption that the second-order nonlinearity varies stepwise along the length of the fibre (with a duty ratio of 50%), it can be shown that $\chi^{(2)}_0 = \pi\chi^{(2)}_{\text{eff}}$. Thus, the lower estimate of the maximum second-order nonlinearity in the PPSF sample under consideration is $\chi^{(2)}_0 = 0.016$ pm V^{-1}. Even though this $\chi^{(2)}_0$ value is a factor of 30 lower than the maximum possible value for silica glass ($\chi^{(2)}_{\text{max}} \approx 0.6$ pm V^{-1}), this PPSF sample can be used in comparative SHG experiments with different fibre configurations.

One way of improving SHG efficiency is by increasing the pump power. In the undepleted-pump regime, this causes the second-harmonic power to rise quadratically. In this study, to raise the power we used for the first time an external fibre cavity, with a PPSF sample placed in it.

4. External cavity SHG in a PPSF

To study external cavity SHG, we used a ring cavity for pump light (Fig. 5). The cavity was formed by connecting ports of a 50/50 fibre coupler and a wavelength-division multiplexing (WDM) coupler, which separated the pump light and second harmonic. The scheme contains two fibre polarisation controllers for matching the pump polarisation at the input with that after a cavity round trip and for matching the pump polarisation with the direction of the principal axes of the PPSF. For phase sweeping, the cavity included a fibre segment that was cemented to a piezoceramic and allowed the cavity length to be varied. The fundamental and second-harmonic powers were measured by photodetectors (PD1 and PD2) behind an empty output port of the WDM coupler, after the beams had been separated by mirrors.

Pump power enhancement in a ring cavity is known to be greatest when the optical loss in the input coupler, which ensures feedback, is equal to the total optical loss in the other components of the cavity [20]. In our case, the measured total loss in the components of the cavity was 3.6 dB, so a 50/50 coupler (3-dB loss) was chosen as a nearly optimal input coupler.

When a sawtooth voltage was applied to the piezoceramic, the external ring cavity operated as a scanning interferometer. In our experiments, we measured transmission spectra of the cavity, i.e. the pump and second-harmonic powers as functions of cavity length, which varied linearly with time (Fig. 6). The experimental data thus obtained are well represented by a theoretical dependence which can be described by the Airy formula for a ring resonator:

$$\eta = \frac{P_{\text{intr}}}{P_{\text{in}}} = \frac{T_1}{(1-\sqrt{T_1T_2})^2 + 4\sqrt{T_1T_2}\sin^2(\delta/2)}, \qquad (5)$$

where η is the external cavity pump power enhancement factor; P_{intr} and P_{in} are the pump powers in the cavity and at the cavity input, respectively; T_1 is the transmission of the input

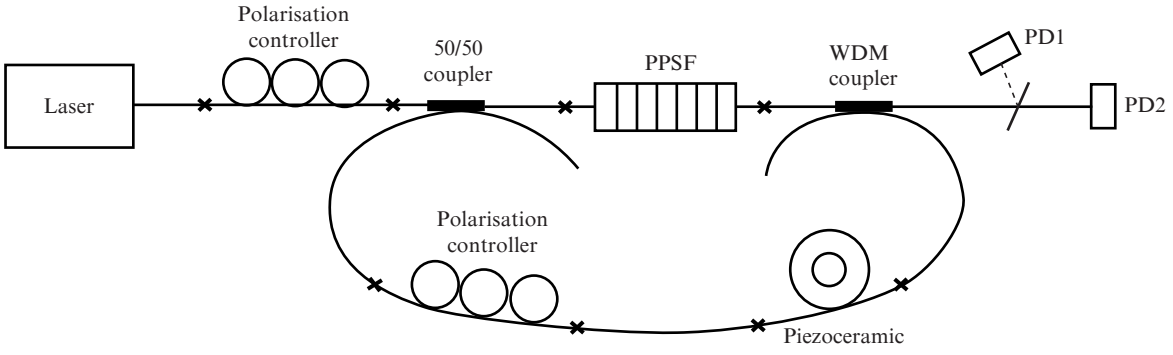

Figure 5. Schematic of the experimental setup used to investigate external cavity SHG in a PPSF.

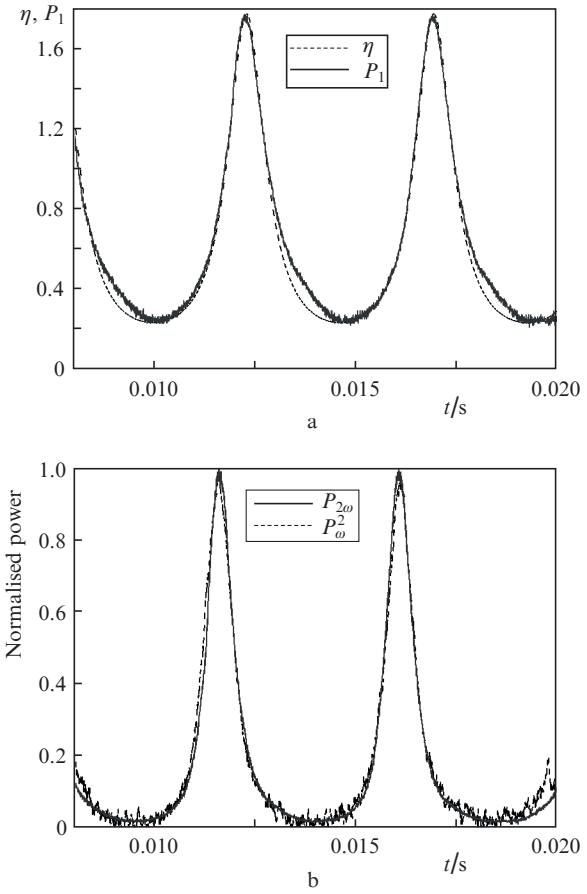

Figure 6. (a) Theoretically predicted and measured transmission spectra of the external fibre cavity for pump light; (b) time variations of the pump (P_ω^2) and second-harmonic ($P_{2\omega}$) powers at the cavity output.

coupler; T_2 is the transmission of the rest of the cavity; and δ is the cavity round trip phase shift.

The best fit cavity pump power enhancement factor η is 1.8 (Fig. 6a). Note that the asymmetric broadening in the bottom part of the measured spectrum in comparison with the theoretically predicted one can be accounted for by the effect of an additional polarisation mode. The relatively small pump power enhancement is associated with the high cavity loss (3.6 dB), which is contributed mainly by the loss in the fusion splices between the PPSF and the standard single-mode fibres. We believe that optimising the splice loss and reducing the cavity loss to a level of 0.5 dB will allow the fundamental power in the cavity to be raised by ten times.

The second-harmonic power measured at the output of the cavity varies quadratically with the pump power in the ring cavity. Figure 6b shows the normalised second-harmonic power $P_{2\omega}$ as a function of cavity length, which varies linearly with time. It is seen that the dependence, measured directly, is essentially identical to that of P_ω^2 (P_ω was evaluated from the IR transmission spectrum of the cavity). The noise contamination in the dependence of the second-harmonic power on cavity length is caused by the low power level.

The use of an external cavity with a pump power enhancement $\eta = 1.8$ should, in theory, ensure an increase in second-harmonic power by $\eta^2 \approx 3.2$. However, the experimentally determined increase in second-harmonic power was by about a factor of 2. In our experiments, we compared external cavity SHG in the PPSF and single-pass SHG with no 50/50 fibre coupler (Figs 5 and 3, respectively) at the same power of the fundamental single-frequency light ($P_{in} \approx 600$ mW in both cases). One possible reason for the smaller experimentally determined increase in second-harmonic power is that not all the pump light accumulated in the cavity is linearly polarised along the X axis in the PPSF. Pump light polarised along the Y axis of the PPSF is converted into the second harmonic with an efficiency a factor of $(\chi^{(2)}_{XXX}/\chi^{(2)}_{XYY})^2 = 9$ lower than the conversion efficiency for pump light polarised along the X axis. In subsequent experiments, we will be able to eliminate this effect using polarisation-maintaining fibres.

5. Conclusions

We have studied frequency doubling of a cw single-frequency ytterbium-doped fibre laser directly in a periodically poled silica fibre. SHG in a fibre sample inserted into an external fibre cavity has been studied for the first time. The results demonstrate that the high level of losses in the PPSF at the fundamental frequency allows one to obtain a relatively small second-harmonic power enhancement (~2) in the external cavity scheme. Using polarisation-maintaining fibres and reducing the cavity loss to a level of 0.5 dB, one can increase the fundamental mode power in the cavity by about ten times and, accordingly, reach a second-harmonic power of several milliwatts at a pump power of ~1 W, with $P_{2\omega}$ scaling quadratically with pump power P_ω and/or $\chi^{(2)}_{eff}$.

Acknowledgements. We are grateful to M.A. Nikulin for supplying the single-frequency DFB laser and E.A. Zlobina for her assistance in the characterisation of the samples. This work was supported by the Russian Science Foundation (Project No. 14-22-00118) and the Russian Academy of Sciences.

References

1. Akulov A.V., Kablukov S.I., Babin S.A. *Kvantovaya Elektron.*, **42**, 120 (2012) [*Quantum Electron.*, **42**, 120 (2012)].
2. Kontur E.J., Dajani J., LuYalin, Knize R.J. *Opt. Express*, **20**, 12882 (2007).
3. Kazansky P.G., Pruneri V. *J. Opt. Soc. Am.*, **11**, 3170 (1997).
4. Kashyap R., in *Fiber Bragg Gratings* (New York: Acad. Press, Elsevier, 2010).
5. Weber M.J. *Handbook of Optical Materials* (Boca Raton: CRC Press, 2003).
6. Canagasabey A., Corbari C., Zhang Z., Kazansky P.G., Ibsen M. *Opt. Lett.*, **32**, 1863 (2007).
7. Canagasabey A., Corbari C., Gladyshev A.V., Liegeois F., Guillemet S., Hernandez Y., Yashkov M., Kosolapov A., Dianov E.M., Ibsen M., Kazansky P.G. *Opt. Lett.*, **34**, 2483 (2009).
8. Corbari C., Gladyshev A.V., Lago L., Ibsen M., Hernandez Y., Kazansky P.G. *Opt. Lett.*, **22**, 6505 (2014).
9. Lim E.L., Corbari C., Gladyshev A.V., Alam S.U., Ibsen M., Richardson D.J., Kazansky P.G., in *Top. Meeting Bragg Gratings, Poling Photosensitivity 2014* (Barselona, 2014) Paper JTu6A.5.
10. Dvoyrin V.V., Gladyshev A.V., Mashinsky V.M., Dianov E.M., Canagasabey A., Corbari C., Ibsen M., Kazansky P.G., in I*EEE ECOC 2008* (Brussel, 2008) Vol. 2-5, paper Tu.1.B.1.
11. Dontsova E.I., Kablukov S.I., Babin S.A. *Kvantovaya Elektron.*, **43**, 467 (2013) [*Quantum Electron.*, **43**, 467 (2013)].
12. Telford W.G., Babin S.A., Khorev S.A., Rowe S.H. *Cytometry A*, **12**, 1031 (2009).
13. Ghosh G., Yajima H. *J. Lightwave Technol.*, **16** (11), 2002 (1998).
14. Gloge D. *Appl. Opt.*, **10** (10), 2252 (1971).
15. Gladyshev A.V., Corbari C., Medvedkov O.I., Vasiliev S.A., Kazansky P.G., Dianov E.M. *J. Lightwave Technol.*, **33**, 439 (2015).

16. Nikulin M.A., Babin S.A., Dmitriev A.K., Dychkov A.S., Kablukov S.I., Lugovoy A.A., Pecherskii Yu.Ya. *Kvantovaya Elektron*., **39**, 906 (2009) [*Quantum Electron*., **39**, 906 (2009)].
17. Zhu E.Y., Quan Li, Liscidini M., Sipe J.E., Corbari C., Canagasabey A., Ibsen M., Kazansky P.G. *Opt. Lett*., **10**, 1530 (2010).
18. Dontsova E.I., Lobach I.A., Dostovalov A.V., Kablukov S.I. *Prikl. Fotonika*, **4**, 342 (2015).
19. Lobach I.A., Kablukov S.I., Podivilov E.V., Babin S.A. *Opt. Express*, **18**, 17632 (2011).
20. Risk W., Gosnell T., Nurmikko A. *Compact Blue-Green Lasers* (Cambridge: Cambridge University Press, 2003) p. 551.